Biosensors and Bioelectronics 132 (2019) 203–209

Contents lists available at ScienceDirect

Biosensors and Bioelectronics

journal homepage: www.elsevier.com/locate/bios

Electroluminescent aptasensor based on $RuSiO_2$ nanoparticles for detection cytochrome c using ferrocene as quenching probe

Haifeng Sha[a], Yao Zhang[a], Yinfang Wang[a], Hong Ke[a], Xin Xiong[a], Huaiguo Xue[b], Nengqin Jia[a,*]

[a] The Education Ministry Key Laboratory of Resource Chemistry, Shanghai Key Laboratory of Rare Earth Functional Materials, College of Chemical and Materials Science, Shanghai Normal University, Shanghai 200234, PR China

[b] College of Chemistry & Chemical Engineering, Yangzhou University, Yangzhou 225002, China

ARTICLE INFO

Keywords:
Electrochemiluminescence
$Ru(bpy)_3^{2+}$-doped silica nanoparticles
Fc-aptamer
Cytochrome c

ABSTRACT

A stable sandwiched electrochemiluminescence (ECL) aptasensor was originally constructed established upon $Ru(bpy)_3^{2+}$-doped silica nanoparticles ($RuSiO_2$ NPs) with ferrocene carboxylic acid-aptamer (Fc-aptamer) to quantitatively detect cytochrome c (Cyt C). Herein, $RuSiO_2$ NPs and Fc-aptamer were respectively prepared through the microemulsion method and amide reaction to fabricate the ECL aptasensor. Furthermore, Fc-aptamer was used as quenching probe for quenching the ECL emission of $RuSiO_2$ NPs. In detail, $RuSiO_2$ NPs were primarily immobilized onto the electrodes by the film-forming function of chitosan. Subsequently, the aptamer was incubated onto the decorated GCE via crosslinking with glutaraldehyde (GA). After Cyt C was connected to the GCE via immunoreaction, Fc-aptamer was immobilized onto the modified electrodes owing to the specific recognition between antigens and aptamer. Ultimately, ECL signals markedly descended owing to the poor electricity conductivity of proteins and superior quenching effect of Fc-aptamer. Under optimum conditions, the designed ECL aptasensor indicated an accurate analysis for Cyt C in a rang of 0.001–100 nM with a detection limit of 0.48 pM (S/N = 3).

1. Introduction

As a significant mitochondrial protein, cytochrome c is the electron deliverer between its reductase and oxidase (Muzyka, 2014). During recent decades, several investigators have found that cytochrome c has an extremely important effect on cell apoptosis. For example, Cain K et al. firstly reported that it is an apoptosis protease-activating factor which is a pivotal element to the proliferation of apoptotic signals in a variety of apoptotic pathways (Cain et al., 2002). Lately, with the further study on the energy metabolism regulation to the apoptosis process, researchers have a clearer understanding about cytochrome c. Normally, Cyt C will release to the cytoplasm to stimulate apoptosis, so it can be served as the early signs of cell apoptosis (Yin et al., 2015). Under pathological conditions, the excessive cytochrome c will enter the bloodstream, which is closely related to certain diseases at the cellular level (Manickam et al., 2017). Moreover, the normal concentration of cytochrome c in human serum is lower than 2 nM (Shamsipur et al., 2017). Therefore, the detection of Cyt C can be used not only as a biomarker of apoptosis, but also as an important factor in studying certain diseases of the cell level (Karimi Pur et al., 2018). So far, various approaches have been utilized to quantify Cyt C, including cyclic voltammetry (Fuku et al., 2012), chemiluminescence (Li et al., 2010), electrochemical impedance spectroscopy (Shafaat et al., 2018) and fluorescence (Salehnia et al., 2017), etc. Aptamer is single-stranded oligonucleotides with tens of nucleotides which have been used in numerous fields due to its characteristics of high specificity, high affinity, and abundant targets (Wu et al., 2015). Moreover, as a novel molecular recognition component, aptamer has the advantages of good thermal stability, long-term infinite preservation, no immunogenicity, uniform activity, and no need for experimental animals compared with traditional antibodies and enzymes (Sun et al., 2014). Accordingly, aptamers are extremely beneficial for the fabrication of biosensing platform owing to their simple synthesis, high stability and easy to modification (Meng et al., 2016). Therefore, they are also considered promising alternatives to antibodies, especially in the detection of proteins.

In particular, ECL technology have received increasing attention as a result of the significant advantages of combining electrochemistry methods with chemiluminescence spectroscopy these years (Karimi Pur et al., 2018). Hence, ECL aptasensors have been extensively employed for immunoassay owing to their excellent sensitivity, prominent specificity, satisfactory accuracy and simple operation (Li et al., 2017). For

* Corresponding author.
E-mail address: nqjia@shnu.edu.cn (N. Jia).

https://doi.org/10.1016/j.bios.2019.03.004
Received 28 November 2018; Received in revised form 1 March 2019; Accepted 1 March 2019
Available online 06 March 2019
0956-5663/

example, Motaghi H et al. employed the aptamer modified bipolar electrodes combined with ECL technique to detect human breast cancer cells (Motaghi et al., 2018). During multifarious combination of co-reactants and luminescent reagents, the $Ru(bpy)_3^{2+}$-TPA co-reacting system is frequently utilized for immunoassay in virtue of high fluorescence quantum yield, good biocompatibility, and excellent stability (Ke et al., 2017). Previously, the generally-used means for immobilizing $Ru(bpy)_3^{2+}$ is nafion cation exchange membrane method. However, this way is not only time-consuming, but also reagent-consuming. Furthermore, the luminescent reagent fixed by this method is easy to fall off. In recent years, numerous nanomaterials were applied in immobilizing $Ru(bpy)_3^{2+}$ to heighten ECL signals, including metal organic frameworks (MOFs) (Yuan et al., 2015), polyamidoamine dendrimer (PAMAM) (Babamiri et al., 2018), metal nanomaterials (Ge et al., 2015), and silica nanoparticles (SiO_2 NPs) (Zhou et al., 2015). There are usually two ways: one is to encapsulate $Ru(bpy)_3^{2+}$ in the process of directly forming nanomaterials; the other is to combine nanomaterials with $Ru(bpy)_3^{2+}$ to form a composite. Among these nanomaterials, SiO_2 nanoparticles (NPs) aroused researchers' great concern due to their unique characteristics (Shanthil et al., 2017). For instance, Zhang et al. found that $RuSiO_2$ NPs could not only maintain the property of $Ru(bpy)_3^{2+}$, but also keep it from escaping and dissolving in solution (Zhang and Dong, 2006). Therefore, $RuSiO_2$ NPs showed excellent performance in the construction of electrochemiluminescence sensor. For example, Zhang et al. synthetized Ru@SiO_2 NPs acted as a signal probe for sensitively detecting fumonisin B_1 (Zhang et al., 2017). Besides, ferrocene (Fc) and its derivatives are common and efficient luminescent quenchers for a majority of luminescent materials, such as $Ru(bpy)_3^{2+}$ and its derivative, persulfate system, quantum dots, and metal nanoclusters. As an example, Zhuo et al. prepared ferrocene-graphene nanosheets to effectually quench the luminescence signal of $Ru(bpy)_3^{2+}$ derivative for detecting thrombin (Zhuo et al., 2015).

Consequently, a novel quenching ECL sensor between $RuSiO_2$ nanoparticles and Fc-aptamer composites is fabricated for sensitively detecting cytochrome c. Herein, $RuSiO_2$ NPs and Fc-aptamer were synthesized via the microemulsion method and amide reaction respectively. Compared with the traditional adsorption-fixation method, the strategy of directly encapsulating $Ru(bpy)_3^{2+}$ in the process of synthesizing SiO_2 nanoparticles can greatly improve the stability of the constructed sensor. In addition, Fc-aptamer, acted as effective ECL quencher, can remarkably quench the ECL intensity of $RuSiO_2$ NPs. Therefore, Cyt C can be accurately and sensitively detected by this proposed ECL aptasensor.

2. Experimental sections

2.1. Reagents and materials

Cytochrome C, tris(2,2′-bipyridyl)-dichlororuthenium(II) hexahydrate ($Ru(bpy)_3Cl_2{\cdot}6H_2O$), tripropylamine (TPA), ferrocene carboxylic acid (Fc-COOH), 1-Ethyl-3-(3-dimethylaminopropyl) carbodiimid (EDC), N-hydroxysuccinimide (NHS), bovine serum albumin (BSA, 99%), Tween-20 and chitosan (Chi) were ordered from Sigma – Aldrich (China). The aptamer sequence of cytochrome c (5′-CCGTGTCTGGGG CCGACCGGCGCATTGGGTACGTTGC$(CH_2)_6$-NH_2–3′) was gained from Sangon Biotech (China). Tetraethyl orthosilicate (TEOS) was gained by Sinopharm Reagent (Beijing, China). Triton X-100 (TX-100), n-hexanol and cyclohexane were supplied by Damas-beta (Shanghai, China). The human serum samples were provided by Ruijin Hospital, Shanghai Jiaotong University School of Medicine and kept in −20 °C.

2.2. Experimental instruments

Electrochemical impedance spectroscopy (EIS) and cyclic voltammetry (CV) were carried out via a CHI 760B electrochemistry workstation (Shanghai CH Apparatus Inc, China). The morphology characterization of $RuSiO_2$ NPs was obtained from the scanning electron microscopy (FMSEM, LEO1530 field emission, Germany). UV–vis absorption spectra was tested by a Thermo Multiskan spectrum spectrophotometer. ECL analysis was measured by MPI-E ECL analyzer (Xi'an Remax Electronic High-Tech Ltd.). In addition, a traditional three electrode system was used throughout ECL experiments, including differently modified glassy carbon electrode (working electrode), a Pt wire (counter electrode) and Ag/AgCl (reference electrode).

2.3. Synthesis of $RuSiO_2$ nanoparticles

In this protocol, $RuSiO_2$ nanoparticles were prepared based on the reported method with some changes (Zhang et al., 2017). 1.77 mL TX-100, 7.5 mL cyclohexane, 1.8 mL n-hexanol were mixed in a beaker, then 340 μL $Ru(bpy)_3^{2+}$ solution (7.84 mM) was put into above solution and stirred for 30 min. Afterwards, 100 μL TEOS was placed to the mixture before 60 μL $NH_3{\cdot}H_2O$ (25%) was added quickly. After stirring for 24 h, massive $Ru(bpy)_3^{2+}$ molecules have been encapsulated during the forming process of silica nanoparticles. Ultimately, acetone was used to precipitate the $RuSiO_2$ nanoparticles, then washed alternately with ethanol and water.

2.4. Preparation process of Fc-aptamer

The synthetic method of Fc-aptamer composite material was succinctly and clearly exhibited in Scheme 1. In the beginning, 1 mL mixture of 20 mM EDC and 10 mM NHS was placed in 1 mL 15 μM aptamer. Then, 15 mg Fc-COOH was put in the above solution for ultrasonic agitation 1 h and oscillation 8 h. Eventually, the desired product was collected by centrifugal washing and re-dissolved in the PBS buffer (pH =7.0) for following experiments.

2.5. Construction of the immunosensor

Initially, the polishing treatments of electrodes were carried out by Al_2O_3 powder with the size of 0.3 and 0.05 μm in succession. After rinsing by double distilled, the pretreated electrode was cleaned with ultrasound 3 min and dried by nitrogen. Subsequently, 5 μL $RuSiO_2$ NPs (5 mg/mL) was dropped on every electrode and dried at ambient condition. After that, 5 μL chitosan was covered onto modified electrodes dried at room temperature, and then 5 μL GA (12.5%) was employed in activating amino-group of chitosan for 1 h at 4 °C. After rinsing gently by PBS, 5 μL Cyt C aptamer (15 μM) could be immobilized on the GCE via crosslinking reaction between amino groups in 4 °C. Then, the electrodes were washed softly and added with 3 μL BSAT solution (0.5% BSA containing 1% Tween-20) for 30 min to significantly reduce the impact of nonspecific adsorption. Through rinsing lightly, these well-prepared GCE was incubated by different concentrations of Cyt C via immune recognition reaction in 4 °C. Afterwards, the modified GCE was rinsed by PBS and coated with BSAT respectively. Later, 5 μL as-

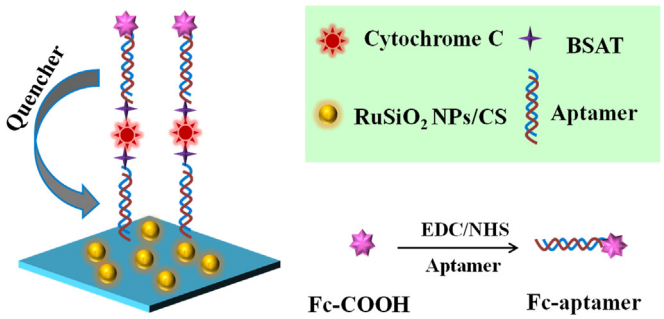

Scheme 1. The fabrication procedures of this proposed sandwich-type electrochemiluminescence aptasensor.

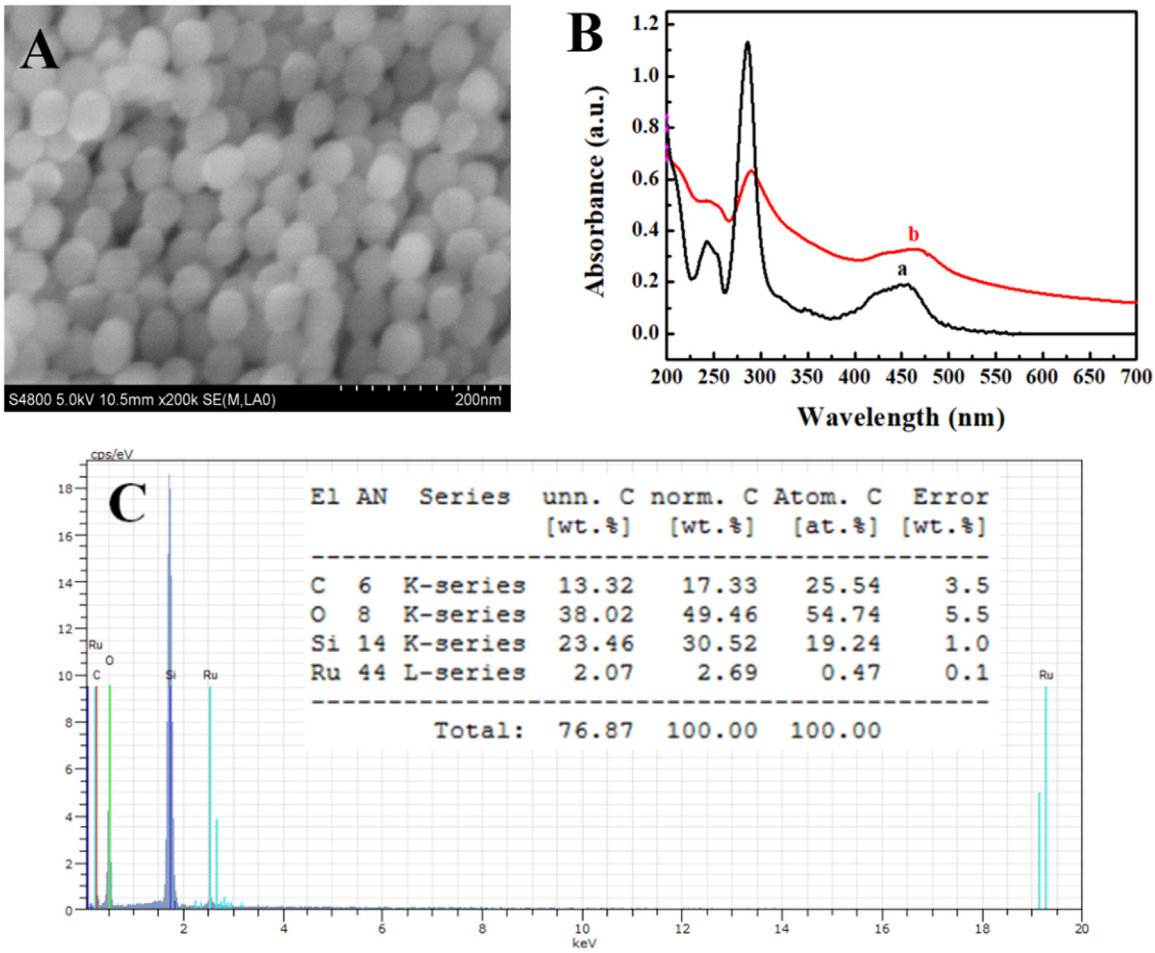

Fig. 1. FMSEM (A) and EDS (C) images of $RuSiO_2$ NPs. (B) UV–Vis absorption spectra of (a) $Ru(bpy)_3^{2+}$ solution and (b) $RuSiO_2$ NPs solution.

prepared Fc-aptamer composites were linked to the acquired ECL sensors via specific immunoreaction in 4 °C. After that, the constructed ECL sensors should be stored in 4 °C before use. Correspondingly, the assembly procedures and analysis mechanism of this sensor was shown in Scheme 1.

3. Results and discussion

3.1. Quenching mechanism of the ECL aptasensor

In this proposal, an ECL sensor which used $RuSiO_2$ NPs as signal probe and Fc-aptamer as quenching probe was designed to sensitively detect cytochrome c. Herein, the possible quenching processes of Fc-COOH on $Ru(bpy)_3^{2+}$ were as follows:

$$Ru(bpy)_3^{2+} - e^- \rightarrow Ru(bpy)_3^{3+} \quad (1)$$

$$TPA - e^- \rightarrow TPA^{+*} \quad (2)$$

$$TPA^{+*} \rightarrow TPA^{*} + H^+ \quad (3)$$

$$Ru(bpy)_3^{3+} + TPA^{*} \rightarrow Ru(bpy)_3^{2+*} + TPA \quad (4)$$

$$Fc\text{-}COOH - e^- \rightarrow Fc\text{-}COOH^+ \quad (5)$$

$$Fc\text{-}COOH^+ + Ru(bpy)_3^{2+*} \rightarrow Fc\text{-}COOH + Ru(bpy)_3^{3+} \quad (6)$$

$$Ru(bpy)_3^{2+*} \rightarrow Ru(bpy)_3^{2+} + h\nu \quad (7)$$

Firstly, both $Ru(bpy)_3^{2+}$ and TPA occur electrooxidation reaction on electrodes, producing $Ru(bpy)_3^{3+}$ and excited states TPA (TPA^*), respectively (Eq. (1,2,3)). Following that, TPA^* can react with Ru $(bpy)_3^{3+}$, further forming excited states $Ru(bpy)_3^{2+}$ ($Ru(bpy)_3^{2+*}$) (Eq. (4)). Accordingly, an ECL emission which wavelength is about 620 nm will generate after the excited states revert to the ground states (Eq. (7)). Nevertheless, the oxidation reaction of Fc-COOH forms stable $Fc\text{-}COOH^+$ (Eq. (5)) which will react with $Ru(bpy)_3^{2+*}$ to prevent the above reaction (Eq. (6)), further quenching ECL signals of system.

3.2. Characteristics of different nanocomposites

FMSEM was employed to characterize the morphology of synthetic $RuSiO_2$ nanoparticles, exhibited in Fig. 1A. These obtained $RuSiO_2$ NPs are homogeneous spheres with a diameter of about 50 nm. To confirm the as-prepared $RuSiO_2$ NPs, UV–vis absorption spectra is a favorable instrument. As depicted in Fig. 1B, there are two apparent absorption peaks at around 285 and 460 nm in $RuSiO_2$ NPs solution (curve b), which correspond to absorption peaks of $Ru(bpy)_3^{2+}$ solution(curve a), indicating that the $RuSiO_2$ NPs are successfully prepared. Moreover, the EDS analysis of $RuSiO_2$ NPs shows the existence of oxygen, silicon, carbon and ruthenium elements (Fig. 1C), further certifying the success preparation of the $RuSiO_2$ NPs. What's more, as shown in Fig. S1, the $RuSiO_2$ NPs can be evenly coated on the surface of glassy carbon electrode. Besides, for the sake of proving the efficient synthesis of Fc-aptamer, UV–vis absorption spectra and EDS analysis were also applied in illustrating the successful modification of Fc on aptamer. As displayed from Fig. S2, an obvious absorption peak at 275 nm could be distinctly seen with Fc or Fc-aptamer (curve a and b) in contrast to the aptamer (curve c), suggesting that the mixture is successfully synthesized. Furthermore, the EDS image also demonstrates the effective preparation of Fc-aptamer, containing carbon, oxygen, sodium,

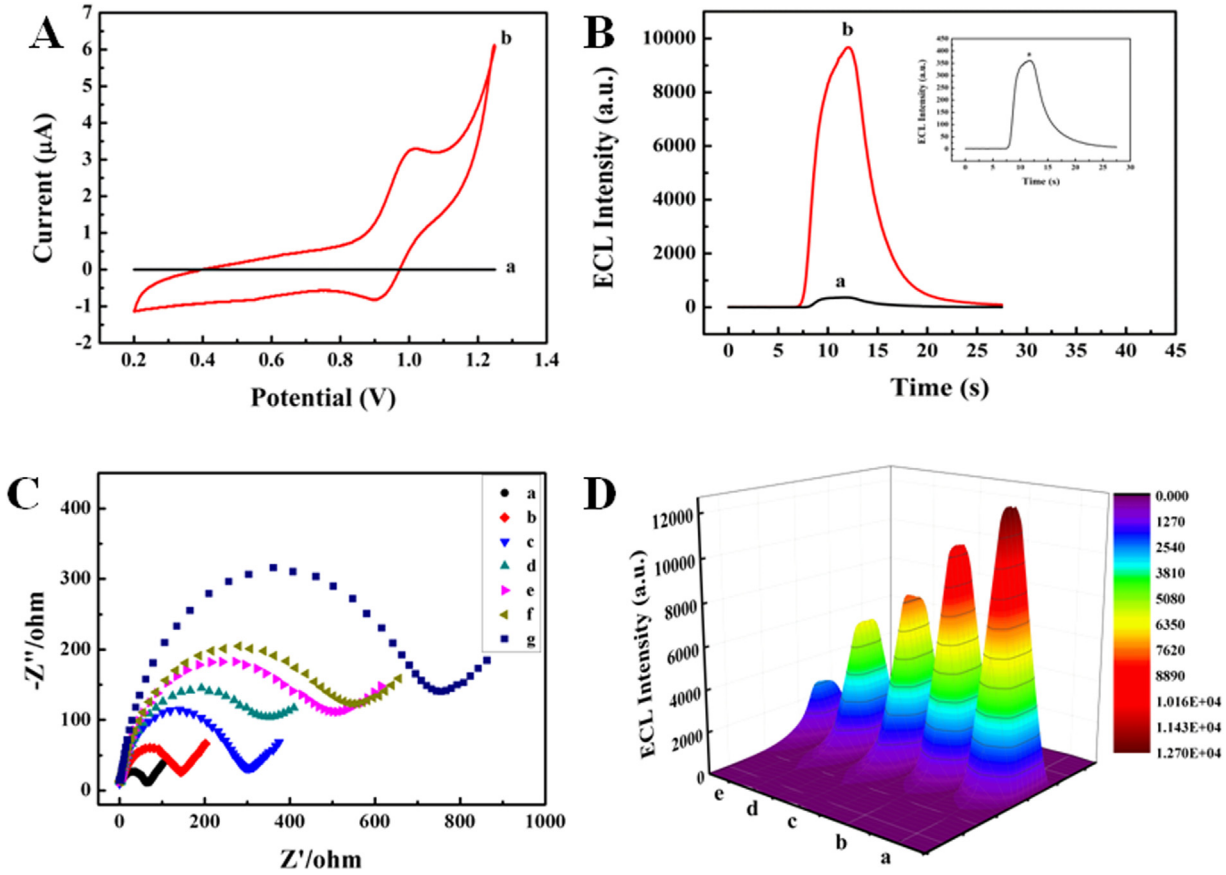

Fig. 2. (A) Cyclic voltammograms of bare GCE (a) and Chi/$RuSiO_2$ NPs/GCE (b) in 0.1 M PBS buffer (pH = 7.0) with 0.5 mM TPA. (B) ECL-time curves of Chi/$RuSiO_2$ NPs modified GCE in 0.1 M PBS buffer (pH = 7.0) without (a) and with 0.5 mM TPA (b). Inset: the magnified curve a. (C) Electrochemical impedance spectroscopy of different decoration of bare GCE (a), Chi/$RuSiO_2$ NPs (b), aptamer (c), BSAT (d), Cyt C (e), BSAT (f) and Fc-aptamer (g) in 0.1 M KCl containing 5 mM $Fe(CN)_6^{3-/4-}$. (D) 3D ECL intensity of successive modification of (a) Chi/$RuSiO_2$ NPs/aptamer, (b) BSAT, (c) Cyt C, (d) BSAT and (e) Fc-aptamer on the GCE in 0.1 M PBS buffer (pH = 7.0) with 0.5 mM TPA.

aluminum, phosphorus, chlorine, potassium and iron elements displayed in Fig. S3.

3.3. Electrochemistry and electrochemiluminescence performances of the aptasensor

In this proposal, cyclic voltammetry, electrochemical impedance spectroscopy and ECL analysis have been applied in investigating the electrode performances of each modified step. As depicted in Fig. 2A, no CV response of bare GCE (curve a) is observed in PBS with 0.5 mM TPA, while a couple of characteristic redox currents of $Ru(bpy)_3^{2+}$ is visible after $RuSiO_2$ NPs were coated on the GCE (curve b), further proving the successful synthesis of $RuSiO_2$ NPs. ECL signals of $RuSiO_2$ NPs remarkably improve in the existence of coreactant, certifying that TPA can dramatically amplify ECL intensities of $Ru(bpy)_3^{2+}$ displayed in Fig. 2B.

Following that, the electronic transfer resistance (Ret) during layer-by-layer assembly processes was measured by the electrochemical impedance spectroscopy. As shown in Fig. 2C, a small resistance value is discovered from the bare GCE (curve a), while the $RuSiO_2$ NPs is coated on the GCE by chitosan (curve b), the Ret becomes bigger, implying that $RuSiO_2$ NPs have a relatively high impedance. The further assembly of the aptamer, BSA, Cyt C and Fc-aptamer greatly increase the Ret (curves c-g) attributed to the protein hindered the electron transfer, suggesting the successful decoration.

Three-dimensional ECL analysis spectroscopy was utilized to explore the ECL signal of stepwise assembling procedure exhibited in Fig. 2D. The ECL intensity of aptamer/Chi/$RuSiO_2$/GCE can be clearly observed from curve a. After BSA and Cyt C were successively immobilized to the modified GCE, the ECL response gradually descend (curves c-d) ascribed to the impede of proteins on electron transport. However, ECL intensities evidently decline (curve e) when Fc-aptamer was modified on the GCE resulting from the outstanding quenching efficiency of Fc-COOH toward the electrochemiluminescence emission of $Ru(bpy)_3^{2+}$, proving that the previously descriptive quenching mechanism is reliable. In addition, the ECL analysis results are consistent with the electrochemical impedance spectroscopy, further corroborating that the layer-by-layer assembly processes are highly successful.

3.4. Optimization of testing conditions for Cyt C

The optimum performances using the constructed ECL aptasensor for quantitative analysis has been obtained by investigating some vital influencing factors, including concentrations of TPA and pH of PBS. As indicated in Fig. 3A, the ECL intensities constantly ascend along with the increased concentration of TPA from 0.1 mM to 0.5 mM, which achieve the maximum at 0.5 mM. Moreover, the ECL intensity modestly declines when the concentration continued to mount up. Accordingly, 0.5 mM as the optimal TPA concentration was used for the next experiments. Besides, as shown in Fig. 3B, effects of pH was also investigated ranged from 6.0 to 8.5 in PBS buffer. The results show that the ECL intensity reaches to the highest point at pH = 7.0. Thus, 7.0 was utilized as the appropriate pH throughout following tests. In optimized conditions, the relative standard deviation (RSD) of this constructed sensor under consecutive ECL scanning for 24 cycles is calculated to be 0.95% displayed in Fig. 3C, indicating the satisfactory stability of this

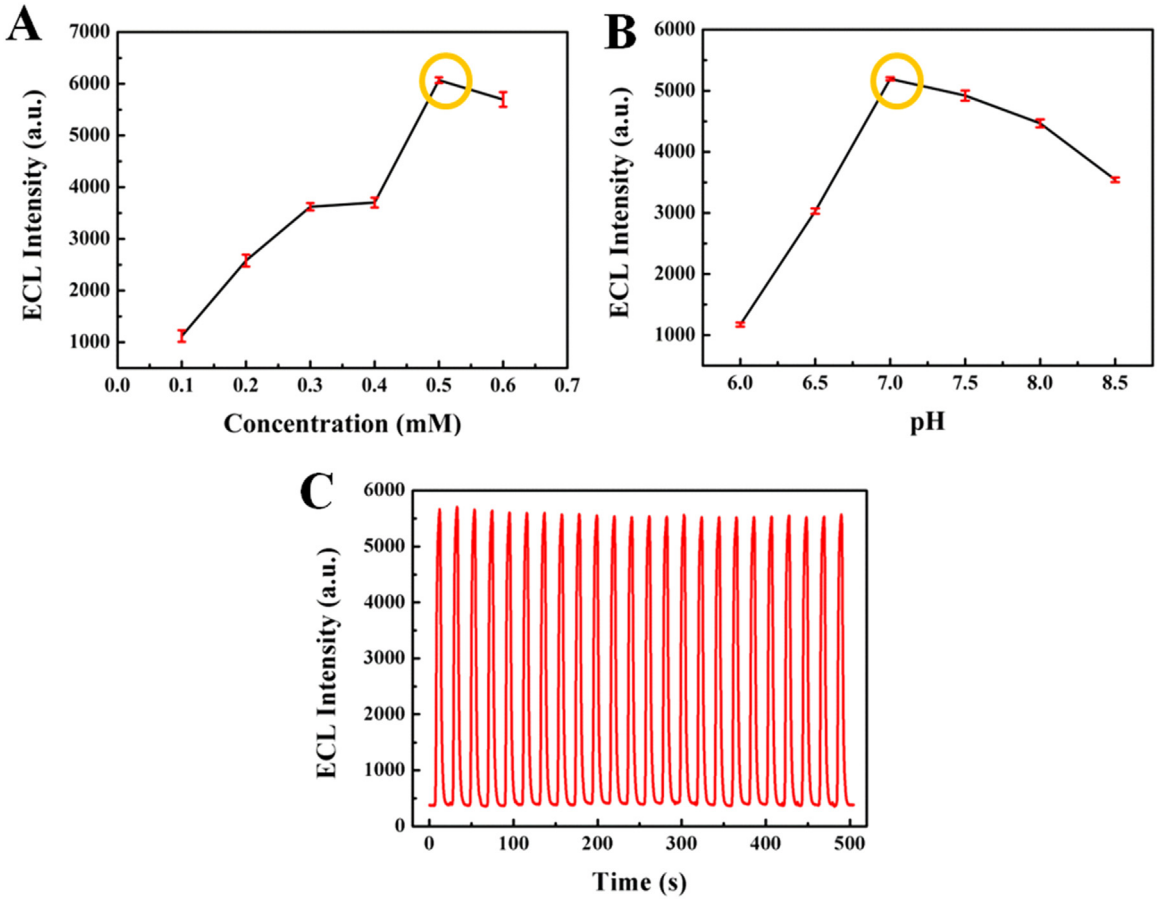

Fig. 3. Influences of (A) concentration of TPA and (B) pH. (C) The ECL signal-time curve of 1.0 nM Cyt C in 0.1 M PBS buffer (pH = 7.0) with 0.5 mM TPA from 0.2 V to 1.2 V for 24 cycles with the scan rate of 100 mV/s.

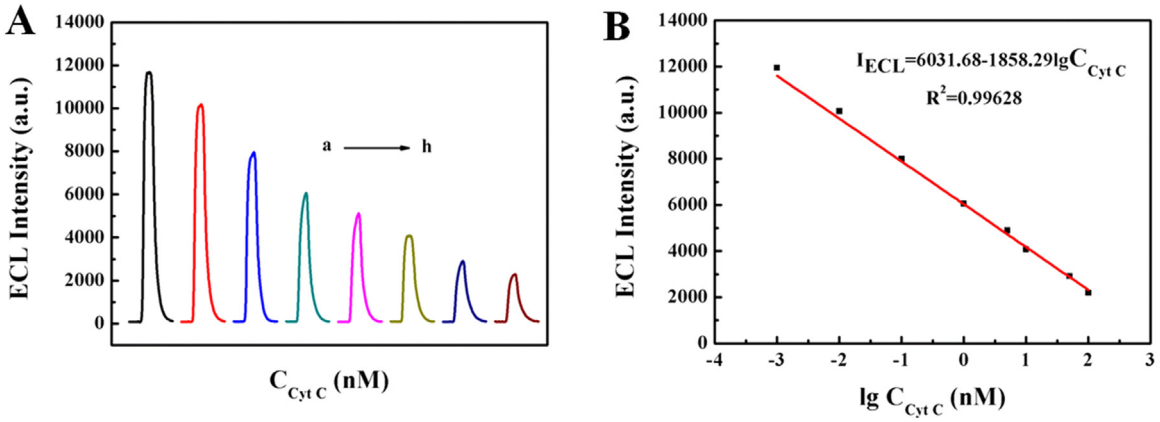

Fig. 4. (A) ECL responses of the proposed ECL aptasensor in 0.1 M PBS buffer (pH = 7.0) with different concentration of Cyt C (nM) from a to h: 0.001, 0.01, 0.1, 1, 5, 10, 50, 100. (B) Calibration curve of the ECL sensor for Cyt C detection with a correlation coefficient (R^2) of 0.99628.

sensor.

3.5. Analytical performances of the designed aptasensor

Quantitative analysis results of this as-prepared ECL aptasensor for Cyt C were gained under the above-mentioned optimum conditions. As depicted from Fig. 4A, prominent decreases of ECL intensities are accompanied with the increases in the concentrations of target ranged from 0.001 to 100 nM (curves a-h). On account of the more target, the more quenching probe Fc-aptamer will be combined. Therefore, the poor electricity conductivity of proteins and strong quenching effect of Fc-aptamer cause together the decline of ECL intensity, which is consistent with the expected mechanism of quantitative results. Meanwhile, a good linear relationship between ECL intensity and logarithm of Cyt C concentrations is depicted in Fig. 4B. Furthermore, the linear regression equation and correlation coefficient (R^2) were respectively correspond to I_{ECL} = 6031. 68–1858.29lg$C_{Cyt\ C}$ and 0.99628. Besides, the detection limit was 0.48 pM by calculation. In addition, the comparison between the designed sensor and previous reported techniques on analyses of target was exhibited in Table S1, illustrating a comparatively lower detection limit and wider linear range of this approach and further suggesting the widespread application prospects of this as-

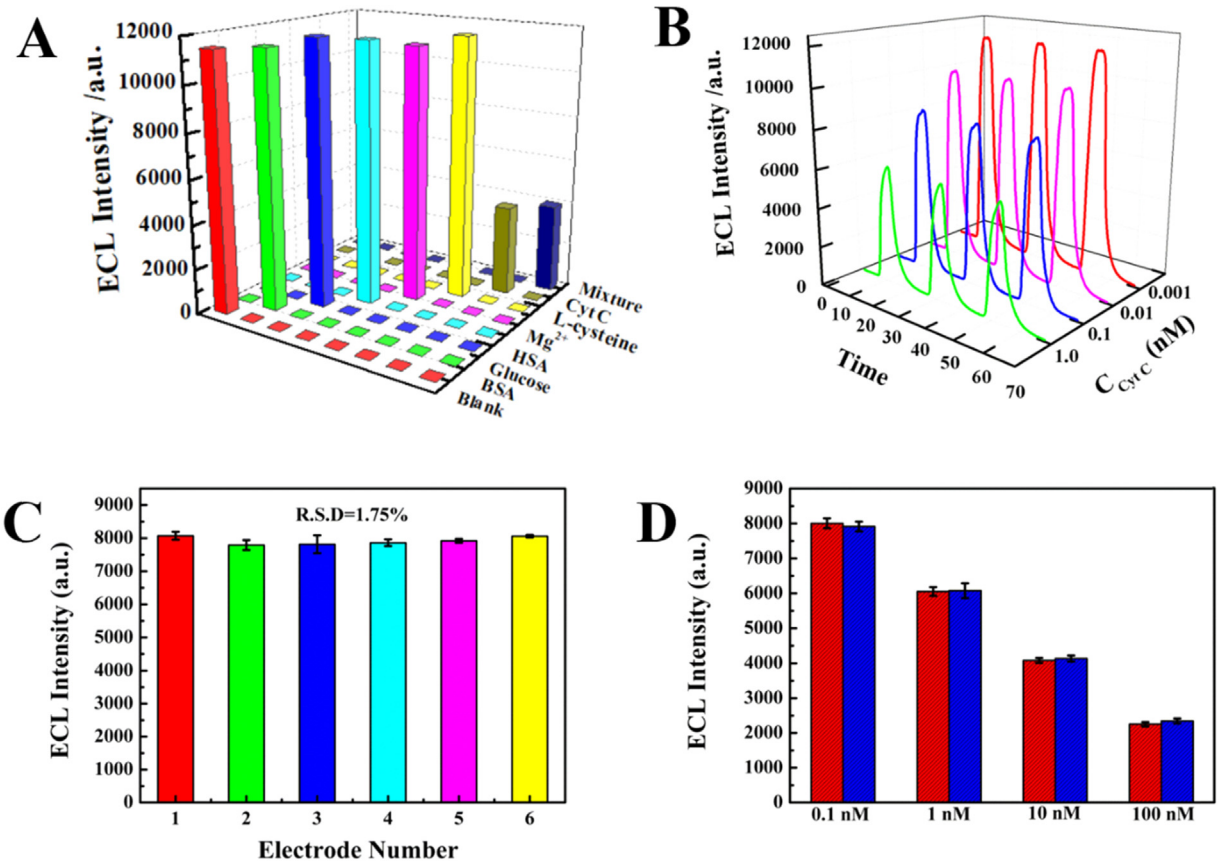

Fig. 5. (A) The specificity of the constructed ECL immunsensor: blank, BSA (10 nM), Glucose (10 nM), HSA (10 nM), Mg^{2+} (10 nM), L-cysteine (10 nM), Cyt C (10 nM), and mixture (10 nM). (B) Stability with different concentration of Cyt C (1.0, 0.1, 0.01, and 0.001 nM) at the ECL aptasensor. (C) Reproducibility inter-assay of the designed ECL aptasensor with six electrodes. (D) Comparison of ECL intensity under different Cyt C concentrations and different conditions (the red one is Cyt C in the PBS, and the blue one is Cyt C in the diluted serum).

prepared ECL sensor on the determination of Cyt C.

3.6. Specificity, stability and repeatability of the aptasensor

Under optimal conditions, to manifest the performances of as-prepared sensor on Cyt C analysis, a series of experiments were performed to study its selectivity, stability and reproducibility. Therefore, 10 nM BSA, Glucose, HAS, Mg^{2+}, L-cysteine, Cyt C and mixture were respectively applied to replace the targets for testifying the specificity of the ECL sensor illustrated in Fig. 5A. Herein, the 0.1 M PBS buffer (pH = 7.0) acted as the blank sample. As a result, the as-prepared sensor has an excellent selectivity to the target. The performance of the developed sensor with various Cyt C concentrations was shown in Fig. 5B, validating the satisfying stability of constructed sensor. Fig. 5C exhibits the ECL responses of six electrodes under the same test conditions. The RSD of six ECL intensities is calculated to be 1.75%, suggesting an acceptable reproducibility for Cyt C analysis using the aptasensor.

3.7. Application of the ECL aptasensor

For the sake of evaluating the practical feasibility of the constructed ECL sensor, the detection of Cyt C in real serum samples was further investigated. Firstly, the human serum was diluted 20 fold with pH7.0 PBS, known quantities of Cyt C were then spiked into 1.0 mL of diluted serum to prepare the actual samples. As clearly shown in Fig. 5D, nearly the same ECL intensity under diverse conditions (red column represents Cyt C in the PBS, blue column represents Cyt C in the diluted serum) indicates that the sensor has potential feasibility in real samples. Furthermore, the recovery rates obtained by standard addition method (Table S2) were ranged from 96.38% to 106.17% with the acceptable RSDs of 1.75–3.48%, indicating the proposed ECL aptasensor is promising for determining Cyt C in real biological samples.

4. Conclusion

In this work, $RuSiO_2$ NPs and Fc-aptamer were respectively synthesized as the signal probe and quenching probe for the fabrication of ECL aptasensor to sensitively detect Cytochrome C. The detection mechanism can be attributed to the excellent quenching of Fc-aptamer towards ECL signals of $RuSiO_2$ NPs. The proposed ECL aptasensor showed favorable analytical performances such as a wide linear range, relatively low detection limit and satisfactory selectivity for the detection of Cyt C, suggesting its great application prospect in the field of biomedical analysis.

CRediT authorship contribution statement

Haifeng Sha: Conceptualization, Formal analysis, Writing - original draft. **Yao Zhang:** Investigation, Data curation. **Yinfang Wang:** Investigation, Data curation. **Hong Ke:** Validation. **Xin Xiong:** Investigation, Data curation. **Huaiguo Xue:** Writing - review & editing. **Nengqin Jia:** Funding acquisition, Supervision, Writing - review & editing.

Acknowledgments

We are grateful for financial support from the Shanghai Science and Technology Committee (17070503000, 18dz2308700), Program for

Changjiang Scholars and Innovative Research Team in University (IRT_16R49) and International Joint Laboratory on Resource Chemistry (IJLRC). Shanghai Engineering Research Center of Green Energy Chemical Engineering.

Declaration of interest statement

The authors declare no competing financial interest.

Credit author statement

Haifeng Sha was responsible for conceptualization, formal analysis and writing - original draft. Yao Zhang, Yinfang Wang and Xin Xiong were in charge of investigation and data curation. Hong Ke performed validation. Huaiguo Xue was responsible for writing - review & editing. Nengqin Jia was in charge of funding acquisition, supervision and writing - review & editing.

Appendix A. Supporting information

Supplementary data associated with this article can be found in the online version at doi.org/10.1016/j.bios.2019.03.004.

References

Babamiri, B., Hallaj, R., Salimi, A., 2018. Ultrasensitive electrochemiluminescence immunoassay for simultaneous determination of CA125 and CA15-3 tumor markers based on PAMAM-sulfanilic acid-Ru(bpy)$_3^{2+}$ and PAMAM-CdTe@CdS nanocomposite. Biosens. Bioelectron. 99, 353–360.

Cain, K., Bratton, S.B., Cohen, G.M., 2002. The Apaf-1 apoptosome: a large caspase-activating complex. Biochimie 84 (2), 203–214.

Fuku, X., Iftikar, F., Hess, E., Iwuoha, E., Baker, P., 2012. Cytochrome c biosensor for determination of trace levels of cyanide and arsenic compounds. Anal. Chim. Acta 730, 49–59.

Ge, L., Su, M., Gao, C., Tao, X., Ge, S., 2015. Application of Au cage/Ru(bpy)$_3^{2+}$ nanostructures for the electrochemiluminescence detection of K562 cancer cells based on aptamer. Sens. Actuators B Chem. 214, 144–151.

Karimi Pur, M.R., Hosseini, M., Faridbod, F., Ganjali, M.R., Hosseinkhani, S., 2018. Early detection of cell apoptosis by a cytochrome C label-Free electrochemiluminescence aptasensor. Sens. Actuators B: Chem. 257, 87–95.

Ke, H., Zhang, X., Guo, W., Zhang, A., Wang, Z., Huang, C., Jia, N., 2017. A MWCNTs-Pt nanohybrids-based highly sensitive electrochemiluminescence sensor for flavonoids assay. Talanta 171, 1–7.

Li, X., Liu, H., He, X., Song, Z., 2010. Determination of cytochrome c in human serum and pharmaceutical injections using flow injection chemiluminescence. Appl. Biochem. Biotechnol. 160 (4), 1065–1073.

Li, Y., Li, Y., Xu, N., Pan, J., Chen, T., Chen, Y., Gao, W., 2017. Dual-signal amplification strategy for electrochemiluminescence sandwich biosensor for detection of thrombin. Sens. Actuators B: Chem. 240, 742–748.

Manickam, P., Kaushik, A., Karunakaran, C., Bhansali, S., 2017. Recent advances in cytochrome c biosensing technologies. Biosens. Bioelectron. 87, 654–668.

Meng, H.M., Liu, H., Kuai, H., Peng, R., Mo, L., Zhang, X.B., 2016. Aptamer-integrated DNA nanostructures for biosensing, bioimaging and cancer therapy. Chem. Soc. Rev. 45 (9), 2583–2602.

Motaghi, H., Ziyaee, S., Mehrgardi, M.A., Kajani, A.A., Bordbar, A.K., 2018. Electrochemiluminescence detection of human breast cancer cells using aptamer modified bipolar electrode mounted into 3D printed microchannel. Biosens. Bioelectron. 118, 217–223.

Muzyka, K., 2014. Current trends in the development of the electrochemiluminescent immunosensors. Biosens. Bioelectron. 54, 393–407.

Salehnia, F., Hosseini, M., Ganjali, M.R., 2017. A fluorometric aptamer based assay for cytochrome C using fluorescent graphitic carbon nitride nanosheets. Microchim. Acta 184 (7), 2157–2163.

Shafaat, A., Faridbod, F., Ganjali, M.R., 2018. Label-free detection of cytochrome C by a conducting polymer-based impedimetric screen-printed aptasensor. New J. Chem. 42 (8), 6034–6039.

Shamsipur, M., Pashabadi, A., Molaabasi, F., Hosseinkhani, S., 2017. Impedimetric monitoring of apoptosis using cytochrome-aptamer bioconjugated silver nanocluster. Biosens. Bioelectron. 90, 195–202.

Shanthil, M., Fathima, H., George Thomas, K., 2017. Cost-effective plasmonic platforms: glass capillaries decorated with Ag@SiO_2 nanoparticles on inner walls as SERS substrates. ACS Appl. Mater. Interfaces 9 (23), 19470–19477.

Sun, H., Zhu, X., Lu, P.Y., Rosato, R.R., Tan, W., Zu, Y., 2014. Oligonucleotide aptamers: new tools for targeted cancer therapy. Mol. Ther. Nucleic Acids 3, e182.

Wu, X., Chen, J., Wu, M., Zhao, J.X., 2015. Aptamers: active targeting ligands for cancer diagnosis and therapy. Theranostics 5 (4), 322–344.

Yin, X., Cai, J., Feng, H., Wu, Z., Zou, J., Cai, Q., 2015. A novel VS_2 nanosheet-based biosensor for rapid fluorescence detection of cytochrome c. New J. Chem. 39 (3), 1892–1898.

Yuan, Q., Zhang, D., Haandel, Lv, Ye, F., Xue, T., Hensen, E.J.M., Guan, Y., 2015. Selective liquid phase hydrogenation of furfural to furfuryl alcohol by Ru/Zr-MOFs. J. Mol. Catal. A: Chem. 406, 58–64.

Zhang, L., Dong, S., 2006. Electrogenerated Chemiluminescence sensors using Ru(bpy)$_3^{2+}$ doped in silica nanoparticles. Anal. Chem. 78 (14), 5119–5123.

Zhang, W., Xiong, H., Chen, M., Zhang, X., Wang, S., 2017. Surface-enhanced molecularly imprinted electrochemiluminescence sensor based on Ru@SiO_2 for ultrasensitive detection of fumonisin B1. Biosens. Bioelectron. 96, 55–61.

Zhou, L., Huang, J., Yu, B., Liu, Y., You, T., 2015. A novel electrochemiluminescence immunosensor for the analysis of HIV-1 p24 antigen based on P-RGO@Au@Ru-SiO_2 composite. ACS Appl. Mater. Interfaces 7 (44), 24438–24445.

Zhuo, B., Li, Y., Huang, X., Lin, Y., Chen, Y., Gao, W., 2015. An electrochemiluminescence aptasensing platform based on ferrocene-graphene nanosheets for simple and rapid detection of thrombin. Sens. Actuators B: Chem. 208, 518–524.